Received: 20 October 2022 | Accepted: 1 November 2022

DOI: 10.1002/pamm.202200325

Optimizing artificial neural networks for mechanical problems by physics-based Rao-Blackwellization: Example of a hyperelastic microsphere model

Gian-Luca Geuken[1], **Jörn Mosler**[1], and **Patrick Kurzeja**[1,*]

[1] Institute of Mechanics, TU Dortmund, Leonhard-Euler-Str. 5, 44227 Dortmund, Germany

The Rao-Blackwell scheme provides an algorithm on how to implement sufficient information into statistical models and is adopted here to deterministic material modeling. Even crude initial predictions are improved significantly by Rao-Blackwellization, which is proven by an error inequality. This is first illustrated by an analytical example of hyperelasticity utilizing knowledge on principal stretches. Rao-Blackwellization improves a 1-d uniaxial strain-energy relation into a 3-d relation that resembles the classical micro-sphere approach. The presented scheme is moreover ideal for data-based approaches, because it supplements existing predictions with additional physical information. A second example hence illustrates the application of Rao-Blackwellization to an artificial neural network to improve its prediction on load paths, which were absent in the original training process.

1 Introduction

Incorporation of physical knowledge into data-driven methods emerged as a promising and yet challenging goal for the description of physical systems. The following references cannot provide a complete overview and must focus on single examples to at least indicate the various research areas involved in this task with a focus on artificial neural networks (ANNs) in material modelling. Elastomeric foams have been investigated by neural networks in [1] and by data-driven constitutive modeling with continuum-mechanics knowledge in a unified network approach in [2]. Information about the physical system can then help to reduce the required data set [3]. The idea of exploiting physical information to reduce the complexity of the problem at hand also relates to ideas from model order reduction, e.g., by training of scale separation [4] or reduced homogenization, e.g., for transient diffusion problems [5]. A hybrid multi-scale approach is used for yield-functions and evolution equations in [6]. [7] and [8] provide a view towards experimental material data with pertinent constraints or parameter identification. Uncertain data and reliability constitute yet another critical aspect, e.g., for the design of artificial neural networks and real-time predictions in tunnel construction [9].

Despite substantial recent developments in employing physical knowledge into ANNs, an improvement of the ANN is usually not granted. For this reason, the present study aims at introducing the concept of Rao-Blackwellization. The so-called Rao-Blackwell(-Kolmogorov) theorem is a statistical tool [10–13]. It nevertheless shares striking methodological similarities with the improvement of ANNs used for deterministic problems. Firstly, Rao-Blackwellization starts from an initial estimator. Secondly, it calls for determination of sufficient information. Thirdly, an algorithm is provided that determines an improved estimator using knowledge about the sufficient information. This task is similar to improving an ANN with sufficient physical information or data. The Rao-Blackwell theorem moreover introduces an error measure by which the improved estimator will be never worse. We will hence adopt the statistical Rao-Blackwell strategy to ANN descriptions of deterministic physical systems. More precisely, the statistical model will be replaced by a physical model. The sufficient statistical information will be replaced by sufficient physical information on the problem at hand. The following analytical and numerical ANN examples aim at providing a simple system to illustrate the strategy, its benefits and open questions. A more detailed background can be found in [14] for application to deterministic multiscale problems.

2 Methodology

Having in mind an ANN for material modeling, we start from an initial prediction θ_0 of an unknown quantity θ (e.g. elastic energy) that depends on physical state $\omega \in \Omega$ (e.g. the strain state). Moreover, we assume from a physical constraint that there is sufficient information $\mathcal{S}$ for the prediction of the unknown. Note that we do not need to know how the exact relationship $\theta(\omega)$ looks like. It is just important to know sufficient information, a small information set is even welcome (e.g. assuming a symmetric strain tensor or rotational invariants for the energy of an isotropic material).

* Corresponding author: e-mail patrick.kurzeja@tu-dortmund.de, phone +49 231 755-5714, fax +49 231 755-2688

The aim is to find a better estimator θ_1 compared to θ_0. Indeed, even crude estimators may lead to a significantly improved one. This is achieved in three steps:

1. Let $\theta_0(\omega)$ be any starting estimator.
2. Let $\mathcal{S}$ be sufficient information to determine θ.
3. Then, the new estimator is

$$\theta_1(s) = \mathbb{A}\left(\theta_0 \,|\, \mathcal{S} = s\right) = \frac{1}{|\Omega_s|}\int\limits_{\Omega_s} \theta_0 \,\mathrm{d}\omega, \quad \Omega_s := \{\omega \in \Omega \,|\, \mathcal{S}(\omega) = s\}, \quad |\Omega_s| := \int_{\Omega_s} 1 \,\mathrm{d}\omega. \tag{1}$$

Ω_s plays a key role. It is the subdomain, where $\mathcal{S}(\omega)$ takes the constant value s. The prediction of θ shall be constant within this subdomain, because its sufficient information is also constant. Rao-Blackwellization enforces this (physically meaningful) behaviour by averaging over this subdomain.

Even more so, the new estimator can be proven to be never worse [10–13] in the sense of the averaged mean squared error between the estimators and the real value of θ

$$\frac{1}{|\Omega|}\int\limits_{\Omega} (\theta_1 - \theta)^2 \,\mathrm{d}\omega \leq \frac{1}{|\Omega|}\int\limits_{\Omega} (\theta_0 - \theta)^2 \,\mathrm{d}\omega, \quad |\Omega| := \int_{\Omega} 1 \,\mathrm{d}\omega. \tag{2}$$

As a first result, the concept of Rao-Blackwellization provides a strategy to incorporate physical knowledge and guarantees to improve our initial prediction in the sense of the averaged error in Eq. (2). The following examples will illustrate these capabilities by means of strain-dependent hyperelastic energies.

3 Analytical Example

This theoretical analysis of a hyperelastic material will show how Rao-Blackwellization can naturally motivate the concept of micro-sphere modeling [15]. The prediction of interest is the elastic energy θ. The impact on ANNs is analyzed later. Statistical considerations of micro-sphere modeling (such as Langevin statistics and random-walk of chain segments) are also omitted for better distinction of physics-based Rao-Blackwellization from statistics-based Rao-Blackwellization. The examples remain purely deterministic.

The initial estimator shall use the stretch of positive-integer powers of the right stretch tensor $\boldsymbol{U}$ in only one direction $\boldsymbol{e}_1$ as

$$\theta_0 = c_0 + c_1\,\boldsymbol{e}_1 \cdot \boldsymbol{U} \cdot \boldsymbol{e}_1 + c_2\,\boldsymbol{e}_1 \cdot \boldsymbol{U}^2 \cdot \boldsymbol{e}_1 + \ldots = \sum_{n=0}^{N} c_n\,\boldsymbol{e}_1 \cdot \boldsymbol{U}^n \cdot \boldsymbol{e}_1. \tag{3}$$

Using only a single stretch direction clearly constitutes a crude initial estimator, despite the approach of involving multiple powers of $\boldsymbol{U}$ (the right Cauchy-Green tensor would be, for instance, $\boldsymbol{C} = \boldsymbol{U} \cdot \boldsymbol{U} =: \boldsymbol{U}^2$). This situation may be understood as a measurement of stretch in a predefined direction, for example, obtained from limited DIC data.

For an isotropic material, we may now assume that sufficient information is provided by knowledge of the principal stretches

$$S = \{\lambda_I, \lambda_{II}, \lambda_{III}\}. \tag{4}$$

Note that they may belong to other directions than $\boldsymbol{e}_1$ of the initial estimator.

With the first two steps of Rao-Blackwellization available (initial estimator and sufficient information), the improved estimator reads

$$\theta_1(\lambda_I, \lambda_{II}, \lambda_{III}) = \mathbb{A}\left(\theta_0 \,|\, \mathcal{S} = \lambda_I, \lambda_{II}, \lambda_{III}\right) = \frac{\int\limits_{\Omega_s(\lambda_I,\lambda_{II},\lambda_{III})} \theta_0 \,\mathrm{d}\omega}{\int\limits_{\Omega_s(\lambda_I,\lambda_{II},\lambda_{III})} 1 \,\mathrm{d}\omega} = \frac{\int_0^{2\pi}\int_0^{\pi} \theta_0 \,\sin\vartheta \,\mathrm{d}\vartheta \,\mathrm{d}\varphi}{\int_0^{2\pi}\int_0^{\pi} 1 \sin\vartheta \,\mathrm{d}\vartheta \,\mathrm{d}\varphi} \tag{5}$$

$$\begin{aligned}
&= \frac{\sum\limits_{n=0}^{N} c_n \int_0^{2\pi}\int_0^{\pi} \Big[\boldsymbol{e}_1 \cdot \boldsymbol{Q}^T(\vartheta,\varphi) \cdot \boldsymbol{U}^n \cdot \boldsymbol{Q}(\vartheta,\varphi) \cdot \boldsymbol{e}_1\Big] \sin\vartheta \,\mathrm{d}\vartheta \,\mathrm{d}\varphi}{4\pi} \\
&= c_0 \frac{1+1+1}{3} + c_1 \frac{\lambda_I + \lambda_{II} + \lambda_{III}}{3} + c_2 \frac{\lambda_I^2 + \lambda_{II}^2 + \lambda_{III}^2}{3} + \ldots \\
&= \sum_{n=0}^{N} c_n \,\frac{\lambda_I^n + \lambda_{II}^n + \lambda_{III}^n}{3} = \sum_{n=0}^{N} c_n \,I_{\boldsymbol{U}^n}.
\end{aligned} \tag{6}$$

It has been used that the states, where the sufficient information of principal stretches $\mathcal{S} = \lambda_I, \lambda_{II}, \lambda_{III}$ remains constant, are just all rotations of the strain state. The hyperelastic energy must not change if the strain state is rotated. We may thus parametrize this set of strain states by rotations $\boldsymbol{Q}$ of $\boldsymbol{U}^n$ and further note that $(\boldsymbol{Q}^T \cdot \boldsymbol{U} \cdot \boldsymbol{Q})^n = \boldsymbol{Q}^T \cdot \boldsymbol{U}^n \cdot \boldsymbol{Q}$.

Incorporating the principal stretches as sufficient information directly dictates an averaging over all strain directions and Eq. (5) resembles the general microsphere averaging concept [15]. Rao-Blackwellization accordingly transforms the specific, crude estimator θ_0 into an average over all principal stretches (cf. Eq. (53) in [15] for the transformation between the second and third line in the above equations). The new estimator in Eq. (6) hence only depends on the principal stretches or on the first invariants $I_{\boldsymbol{U}^n}$, respectively, see Fig. 1 for an illustration.

This example shows that Rao-Blackwellization, when applied to a physical model, has the capability to transform a crude estimator into a physically sound improvement. A discussion on the role of different sufficient statistics or different initial estimators unfortunately exceeds the scope of this treatise. It shall be emphasized that the presented strategy does not always allow to interprete the new estimator on the basis of familiar physical concepts such as the microsphere model. The error inequality in Eq. (2), however, is always guaranteed. The intention of Rao-Blackwellization is also different from proposing classic model descriptions. Instead of developing an entire framework, it just employs an initial estimator (even an improper one is possible) and knowledge about sufficient information on the unknowns (which is the point where the additional physics enter the prediction). This makes it a suitable tool for situations where a complete physical framework is not provided — especially neural networks. The following example will thus demonstrate how neural networks may benefit from Rao-Blackwellization of physical information.

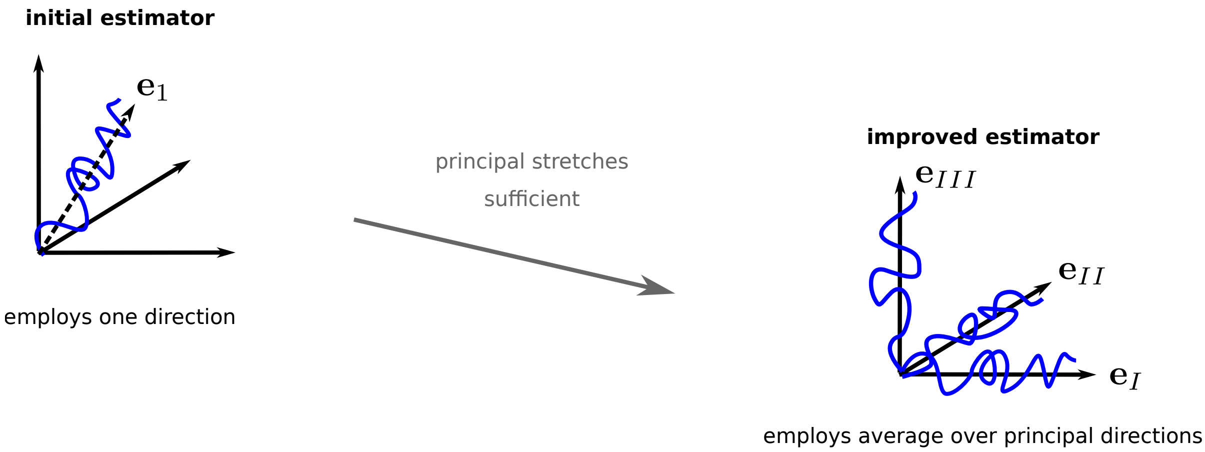

Fig. 1: Illustation of Rao-Blackwellization for a hyperelastic energy based on a single stretch direction. Improvement is due to sufficient information under the assumption of rotational invariance.

4 ANN Example

Elastic energy θ of a hyperelastic material is again considered. In contrast to the previous example, the initial estimator θ_0 is now the prediction made by an ANN. To stay in line with the motivation of the analytical example, this ANN is limited on purpose by considering deformations of the right Cauchy-Green tensor $\boldsymbol{C}$ only in one direction

$$\theta_0 = \text{ANN}\left(\boldsymbol{e}_1 \cdot \boldsymbol{C} \cdot \boldsymbol{e}_1\right) = \text{ANN}\left(C_{11}\right). \tag{7}$$

Note for comparison with literature that a formulation via the left Cauchy-Green tensor $\boldsymbol{b}$ instead of $\boldsymbol{C}$ does not change the following results, because both tensors share the same invariants and principal stretches.

The training and validation data was generated from a compressible Arruda-Boyce model [16] for the sake of illustration

$$\psi = D_1 \left(\frac{J^2 - 1}{2} - \ln(J) \right) + C_1 \sum_{i=1}^{5} \alpha_i \, \beta^{i-1} \left(\bar{I}_1^i - 3^i \right) \tag{8}$$

with deformation gradient $\boldsymbol{F}$, $\boldsymbol{C} = \boldsymbol{F}^T \cdot \boldsymbol{F}$, $J = \det(\boldsymbol{F})$, $I_1 = \text{tr}(\boldsymbol{C})$ and $\bar{I}_1 = I_1 \, J^{-\frac{2}{3}}$. The consistency condition of this material model is fulfilled by resembling the elastic moduli in the linear case. These are based on experimental data for silicone in [17] with a Young's modulus of 1.5 MPa and a Poisson's ratio of 0.49. The obtained material as well as the model parameters are given in Table 1.

Parameter	C_1	D_1	α_1	α_2	α_3	α_4	α_5	β
	$0.4938\,\text{MPa}$	$12.5\,\text{MPa}$	$\frac{1}{2}$	$\frac{1}{20}$	$\frac{11}{1050}$	$\frac{19}{7000}$	$\frac{519}{673750}$	$\frac{1}{49}$

Table 1: Material and model parameters of the Arruda-Boyce model.

To account for the ANN limitation to only one direction, it was trained for data pairs as a parametrization of stretches $\lambda_{11} = 0,\, 0.1,\, 0.2, \ldots,\, 5$ $(\lambda_{22} = \lambda_{33} = 0)$ as

$$C_{11} = (1 + \lambda_{11})^2 \tag{9}$$

$$\psi = D_1 \left(\frac{\lambda_{11}^2}{2} + \lambda_{11} - \ln(1 + \lambda_{11}) \right) + C_1 \sum_{i=1}^{5} \alpha_i\, \beta^{i-1} \left(\left(\frac{\lambda_{11}^2 + 2\lambda_{11} + 3)}{(1 + \lambda_{11})^{\frac{2}{3}}} \right)^i - 3^i \right). \tag{10}$$

Also note that the above energy is not of a simple polynomial format in terms of stretch tensors like in the analytical example above. Neither its ANN approximation nor the subsequent Rao-Blackwellization may thus yield a concise or distinctive series in terms of principal stretches. They will likely result in analytically cumbersome relationships. This situation is nevertheless just beneficial for Rao-Blackwellization. It will guarantee an improved version in the sense of the error inequality, independent of the format of the initial or the improved prediction.

We employ a simple, fully-connected feedforward neural network with three hidden layers each consisting of ten neurons to predict the scalar energy output. The rectified linear unit is used as an activation function for every neuron. The training process is performed via the stochastic gradient descent method with varying batch size and learning rate. The mean absolute percentage error is applied to the loss function and input and output data is preprocessed to avoid singularities from division by zero as well as exploding gradients.

Starting from the crude ANN, we can now set up the improved estimator as follows. Again, we assume an isotropic material such that sufficient information is provided by knowing the eigenvalues or principal stretches, respectively,

$$S = \{\lambda_I, \lambda_{II}, \lambda_{III}\}. \tag{11}$$

Following the Rao-Blackwell procedure, the improved estimator reads

$$\theta_1(\lambda_I, \lambda_{II}, \lambda_{III}) = \frac{\int\limits_{\Omega_s(\lambda_I,\lambda_{II},\lambda_{III})} \theta_0 = \text{ANN}(\boldsymbol{e}_1 \cdot \boldsymbol{C} \cdot \boldsymbol{e}_1)\, \mathrm{d}\omega}{\int\limits_{\Omega_s(\lambda_I,\lambda_{II},\lambda_{III})} 1\, \mathrm{d}\omega}$$

$$= \frac{\int\limits_0^{2\pi} \int\limits_0^{\pi} \text{ANN}\left(\boldsymbol{e}_1 \cdot \boldsymbol{Q}^T(\vartheta, \varphi) \cdot \boldsymbol{C} \cdot \boldsymbol{Q}(\vartheta, \varphi) \cdot \boldsymbol{e}_1 \right) \sin\vartheta\, \mathrm{d}\vartheta\, \mathrm{d}\varphi}{\int\limits_0^{2\pi} \int\limits_0^{\pi} 1 \sin\vartheta\, \mathrm{d}\vartheta\, \mathrm{d}\varphi}. \tag{12}$$

$$\approx \frac{1}{288} \sum_{\substack{\vartheta \in [0,\, \pi/12,\, \ldots,\, \pi] \\ \times \varphi \in [0,\, \pi/12,\, \ldots,\, 2\,\pi]}} \text{ANN}\left(\boldsymbol{e}_1 \cdot \boldsymbol{Q}^T(\vartheta, \varphi) \cdot \boldsymbol{C} \cdot \boldsymbol{Q}(\vartheta, \varphi) \cdot \boldsymbol{e}_1 \right). \tag{13}$$

Since an analytical integration of the ANN is not possible, the improved estimator is approximated by averaging representative directions. In order to obtain these directions both angles are discretized in steps of $\Delta\vartheta = \Delta\varphi = \pi/12$. This might seem quite coarse at first sight but a convergence study showed that it is accurate enough while keeping the computational costs reasonable. Note that the averaging has to be done for every strain state. The computational bottleneck is hence not the evaluation of the ANN but rather rotating the deformation state in the different directions, which still remains an inexpensive operation compared to measurements or simulations of these deformation states.

With the improved estimator θ_1 at hand, four different virtual experiments shall be discussed:

a) uniaxial stretch $\lambda_{11} = 0,\, 0.1,\, 0.2, \ldots,\, 5$ $(\lambda_{22} = \lambda_{33} = 0)$

b) uniaxial stretch $\lambda_{22} = 0,\, 0.1,\, 0.2, \ldots,\, 5$ $(\lambda_{11} = \lambda_{33} = 0)$

c) hydrostatic expansion $\lambda_{11} = \lambda_{22} = \lambda_{33} = 0,\, 0.1,\, 0.2, \ldots,\, 5$

d) simple shear $F_{23} = 0,\, 0.1,\, 0.2, \ldots,\, 5$

Load case a) resembles the data the ANN was trained on. The Rao-Blackwellized ANN output, θ_1, predicts smaller energies than the initial ANN (see Fig. 2 top left). This can be explained by the fact that the initial prediction assumes all stiffness to be oriented in $\boldsymbol{e}_1$-direction, while the improved prediction is a projection onto the microsphere of an isotropic material. Weighting of the other directions is considered evenly for the latter. The improved ANN output accordingly yields better predictions in other directions. Load case b), for instance, is quite similar to load case a). The only difference is that the loading direction is $\boldsymbol{e}_2$ instead of $\boldsymbol{e}_1$. The initial ANN θ_0, however, completely fails to predict a physically meaningful energy and produces a constant zero output. In contrast, the improved version θ_1 fulfills the assumption of an isotropic material and reproduces the same energy as in load case a) (see Fig. 2 top right).

Load case c) is already invariant with respect to rotations. Therefore the initial as well as the improved estimator predict the same energy as has been trained (see Fig. 2 bottom left and compare to θ_0 top left). Load case d) represents a simple shear test in the $\boldsymbol{e}_2 \otimes \boldsymbol{e}_3$ -plane indicated by the component F_{23} of the deformation gradient. Once again, the mere ANN θ_0 fails to predict a physical meaningful energy and produces a constant zero output. And again, the Rao-Blackwellized improvement performs significantly better (see Fig. 2 bottom right).

Finally, the error inequality in Eq. (2) is guaranteed in the sense of an error average over all deformation states. The interpretation of a micro-sphere approach furthermore is also still viable, even though Rao-Blackwellization of the ANN does not allow an insight into the analytical solution. The example clearly demonstrates how neural networks benefit from Rao-Blackwellization of physical information.

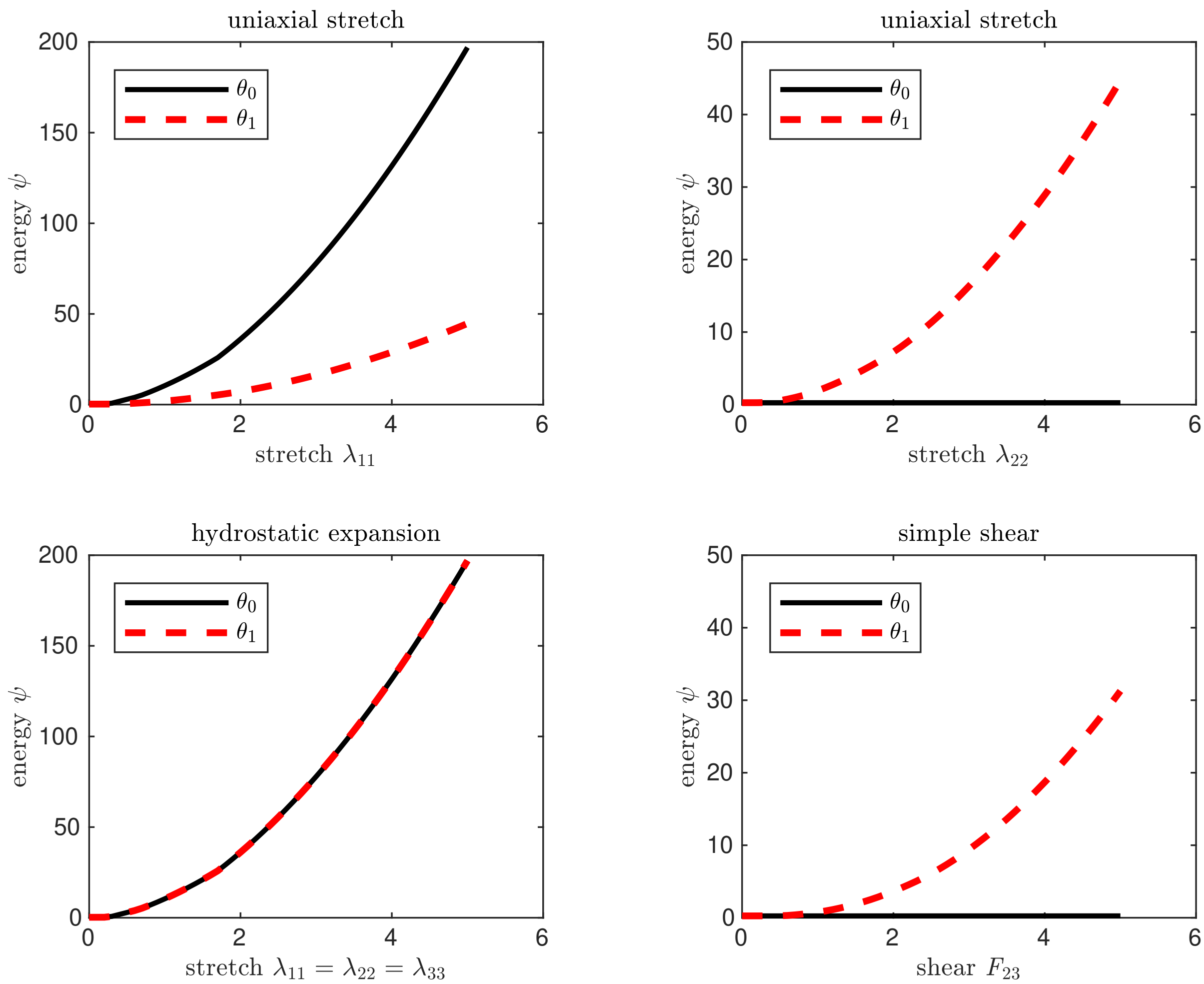

Fig. 2: Comparison of the predicted energy ψ by the initial estimator θ_0 and the improved estimator θ_1 for the four different load cases. The different deformation states are represented on the horizontal axis.

5 Conclusion

The presented analysis showed how the concept of Rao-Blackwellization can be adopted to deterministic physical models and how to utilize it for ANNs. The error inequality and the requirement of sufficient information makes this approach ideal for data-based approaches. Physical knowledge on the system allows to improve even crude initial ANNs. The analytical example demonstrated how Rao-Blackwellization motivated the microsphere concept. The ANN example showed how a physical meaningful prediction for new load paths can be obtained via Rao-Blackwellization, even if the load paths were not part of the training data and also not included in the ANN structure.

Future research will continue with implications for non-academic examples and a mathematical background of the scheme. This will allow a more detailed discussion of the role of parametrizations, the size of sufficient information sets and improvement opportunities for the design of ANNs. It shall be emphasized that there are several other options to adapt neural networks according to the Rao-Blackwell theorem, from mere averaging to generation of artificial training data or improvements of the ANN structure. Inelastic processes such as damage will be studied in particular, utilizing sufficient material and geometric information.

Acknowledgements Open access funding enabled and organized by Projekt DEAL.

References

[1] G. Liang and K. Chandrashekhara, Engineering Structures **30**(7), 2002–2011 (2008).
[2] K. Linka, M. Hillgärtner, K. P. Abdolazizi, R. C. Aydin, M. Itskov, and C. J. Cyron, Journal of Computational Physics **429**, 110010 (2021).
[3] S. Tang, G. Zhang, H. Yang, Y. Li, W. K. Liu, and X. Guo, Computer Methods in Applied Mechanics and Engineering **357**, 112587 (2019).
[4] J. F. Unger and C. Könke, Comput. Struct. **87**(19–20), 1177–1186 (2009).
[5] A. Waseem, T. Heuzé, M. G. Geers, V. G. Kouznetsova, and L. Stainier, Computer Methods in Applied Mechanics and Engineering **380**, 113773 (2021).
[6] C. Settgast, G. Hütter, M. Kuna, and M. Abendroth, International Journal of Plasticity **126**, 102624 (2020).
[7] T. Kirchdoerfer and M. Ortiz, Computer Methods in Applied Mechanics and Engineering **304**, 81–101 (2016).
[8] A. Schowtjak, R. Schulte, T. Clausmeyer, R. Ostwald, A. E. Tekkaya, and A. Menzel, International Journal of Mechanical Sciences **213**, 106840 (2022).
[9] S. Freitag, B. Cao, J. Ninić, and G. Meschke, Computers & Structures **207**, 258–273 (2018), CIVIL-COMP 2017.
[10] D. Blackwell, The Annals of Mathematical Statistics **18**(1), 105–110 (1947).
[11] E. L. Lehmann and G. Casella, Theory of Point Estimation, second edition (Springer-Verlag, New York, NY, USA, 1998).
[12] C. Rao, Linear Statistical Inference and Its Applications, Wiley Series in Probability and Statistics - Applied Probability and Statistics Section Series (Wiley-Interscience, 2001).
[13] P. Bickel and K. Doksum, Mathematical statistics, basic ideas and selected topics, , Vol. 1 (Prentice Hall, New York, NY, USA, 2006).
[14] P. Kurzeja, Proceedings of the Royal Society A: Mathematical, Physical and Engineering Sciences **472**(2189), 20150869 (2016).
[15] C. Miehe, S. Göktepe, and F. Lulei, Journal of the Mechanics and Physics of Solids **52**(11), 2617–2660 (2004).
[16] E. M. Arruda and M. C. Boyce, Journal of the Mechanics and Physics of Solids **41**(2), 389–412 (1993).
[17] P. Kurzeja, H. Steeb, M. A. Strutz, and J. Renner, The Journal of the Acoustical Society of America **140**(6), 4378–4395 (2016).

